Journal of Luminescence 132 (2012) 2753–2762

Contents lists available at SciVerse ScienceDirect

Journal of Luminescence

journal homepage: www.elsevier.com/locate/jlumin

Luminescence and energy transfer mechanisms in $CaWO_4$ single crystals

D. Spassky [d,*], V. Mikhailin [d], M. Nazarov [a,b], M.N. Ahmad-Fauzi [a], A. Zhbanov [c]

[a] School of Materials and Mineral Resources Engineering, Universiti Sains Malaysia, 14300 Nibong Tebal, Penang, Malaysia
[b] Institute of Applied Physics, Academiei Street 5, Chisinau MD-2028, Moldova
[c] Department of Medical System Engineering, Gwangju Institute of Science and Technology, 1 Oryong-dong, Buk-gu, Gwangju 500-712, Republic of Korea
[d] Skobeltsyn Institute of Nuclear Physics, M.V. Lomonosov Moscow State University, Vorob'evy Gory, 119991 Moscow, Russia

ARTICLE INFO

Article history:
Received 1 March 2012
Received in revised form
10 May 2012
Accepted 18 May 2012
Available online 26 May 2012

Keywords:
Electronic properties
$CaWO_4$
Luminescence
Energy transfer

ABSTRACT

The processes of the excitation energy transfer to the emission centers have been investigated for calcium tungstate crystals taking into account features of the electronic structure of valence band and conduction band. The calculations of the electronic structure of host lattice $CaWO_4$ were performed in the framework of density functional theory. The underestimation of the bandgap value in the calculations has been corrected according to the experimental data. Luminescence of two samples grown using Czochralski (*cz*) and hydrothermal (*ht*) techniques were studied. Intrinsic emission band related to excitons, self-trapped on WO_4 complexes has been observed for the both samples while the additional low-energy emission band related to the defects of crystal structure has been observed only for (*ht*) sample indicating the enhanced concentration of the defects in the sample. It was shown that the features of the conduction band electronic structure are reproduced in the excitation spectrum of intrinsic luminescence only for the (*ht*) sample while for (*cz*) sample the correlation is absent. The enhanced role of the competitive channels in the process of excitation energy transfer to intrinsic emission centers in (*ht*) sample is responsible for the observed difference.

1. Introduction

Calcium tungstate ($CaWO_4$) is a well-known material with attractive luminescence properties. Starting from the end of 19th century when it was used for the registration of X-ray radiation, $CaWO_4$ was extensively used as X-ray phosphor, scintillating material and laser host media. Despite the long history of the utilization, it still finds new areas of application. Recently it was shown that $CaWO_4$ is a perspective material for cryogenic scintillating bolometers, the type of detector that can be used for the search of rare events [1,2].

Because of the long-continued application of $CaWO_4$ its luminescence [3–8] and optical [9–13] properties were studied in details. Less data is available on the band structure of $CaWO_4$. Information about the band structure was initially deduced from the reflectivity spectra measured in the fundamental absorption region which were analyzed using the data of the calculations of molecular orbitals–linear combination of atomic orbitals [10,12,13]. The method allows to ascribe features in the reflectivity to electronic transitions within WO_4 complex, but it does not allow to make certain conclusions about the contribution of the calcium electronic states in the conduction band (CB) and valence band (VB). Only in the last 14 years the calculations of the band structure were performed using different approaches in the framework of the density functional theory (DFT) [14–18]. The calculations allowed getting complete information about the parentage and position of the electronic states in the energy bands of $CaWO_4$. However the calculated data on the band structure depend on the applied calculation method. The verification of the calculations is worth to be performed in this case via the comparison with the experimental data. Optical functions calculated from the data on the density of electronic states can be used for joint analysis with experimental data as it was shown for, $CdWO_4$ [19,20], $PbWO_4$ [21,22], $ZnMoO_4$ [23] and $CaWO_4$ [12]. Underestimation of the bandgap is a problem commonly arising at the calculations of the band structure. The introduction of the self-energy correction [20] or scissors operator [23] at the stage of calculation of optical functions allows to overcome this problem. Simple shift of the permittivity spectra calculated from the data on the band structure with the underestimated bandgap was used in [12] for comparison with the data of experiment for $CaWO_4$. Such procedure is not absolutely correct and it might be one of the reasons for the significant mismatch between the permittivity calculated from experimental data and from the data on the band structure that was obtained for the polarization c//E in [12]. In the present work we are performing joint theoretical and experimental analysis of the band structure of the $CaWO_4$, validating the results of calculations via analysis of permittivity spectra. The bandgap

* Corresponding author. Tel.: +74 95 939 3169.
E-mail address: deris2002@mail.ru (D. Spassky).

0022-2313/$ - see front matter © 2012 Elsevier B.V. All rights reserved.
http://dx.doi.org/10.1016/j.jlumin.2012.05.028

was corrected on the stage of the calculations of the optical functions introducing the scissors operator. It is also considered as a simple and effective method of estimation of a band gap of a given compound.

After certain correction procedure the data on the calculated density of electronic states can be used for analysis of the formation of luminescence excitation spectra as it was shown in [23]. Therefore the data of the calculations were used for the further analysis of the excitation energy transfer to the emission centers in $CaWO_4$. To a considerable degree these processes determine the scintillation light yield that is important for the application of $CaWO_4$ in scintillating bolometers. Two samples of $CaWO_4$ that demonstrate different luminescence properties are under consideration in the present study.

2. Experimental and calculation details

Two test samples of $CaWO_4$ were grown using different techniques. One of the samples was grown using spontaneous crystallization technique from the melt (*ht*) in All-Russia Research Institute of Mineral Materials Synthesis (Russia) while the other was grown using Czochralski technique (*cz*) in I. Franko Lviv National University (Ukraine). Freshly cleaved plane surface was used for the measurements on (*cz*) sample and natural plane surface of growth was used for the measurements on (*ht*) sample. The X-ray phase analysis confirmed the presence of the single tetragonal scheellite phase in both investigated samples. Concentration of impurities in the investigated samples was obtained by means of atomic-emission spectral analysis. The (*cz*) sample contains admixtures of Cl (70 ppm), Fe (20 ppm), Si, K and F (10 ppm) and (*ht*) sample contains admixtures of F, Ni and Mo (10 ppm).

The measurements of emission, luminescence excitation and reflectivity spectra were carried out using synchrotron radiation at the SUPERLUMI station, DESY [24]. McPherson 2-meters primary monochromator equipped with aluminum grating (1200 grooves/mm) allows performing measurements in the energy range 3.7–25 eV with spectral resolution not worse than 0.4 nm. Reflectivity and excitation spectra were corrected using sodium salicilate. Luminescence spectra were measured using Czerny–Turner monochromator "Spectra Pro 300" working in spectrograph mode with CCD detector from Princeton Instruments. Spectra were corrected for the spectral sensitivity of the registration route. Measurements at UV excitation were also carried out at the laboratory set-up of Skobeltsyn Nuclear Physics Institute. Xenon lamp (150 W) was used as a source of excitation and spectra were detected using Oriel MS257 spectrograph equipped with Marconi CCD detector. All presented luminescence spectra were corrected for the spectral sensitivity of the registration route. For the decomposition of the luminescence spectra into elementary components (Gauss distribution) the spectra were converted from nanometer to energy scale. Note that moving from fixed wavelength bandwidth (dW) to energy bandwidth (dE) needs intensity conversion from $I(W)dW$ to $I(E)dE$. For the equivalent conversion the intensity of the luminescence was multiplied on factor λ^2.

The calculations of the electronic structure of $CaWO_4$ host lattice were performed in the framework of DFT. Following Zhang et al. [14] we calculated the electronic structures using theWIEN2k package [25]. WIEN2k is based on the full potential linearized augmented plane wave (LAPW) method, an approach which has proven to be one of the most precise and reliable ways to calculate the electronic structure of solids. The exchange-correlation functional was taken in the generalized gradient approximation (GGA) within the scheme of Perdew et al. GGA96 [26] to determine the total energy, band structure, and density of states (DOS). The lattice parameters and atomic positions of the atoms in $CaWO_4$ were taken from the structural parameters in [27] and the corresponding data are presented in Table 1.

3. Results and discussion

3.1. Band structure calculations

The result of our calculations of band structure is presented in Fig. 1. The obtained result is well correlated with [14]. In order to better describe the strongly correlated 5d electrons of transition metal W the localized density approximation (LDA) and mean-field multi-orbital Hubbard correction, the so-called LDA+U [28] or GGA+U [29] approximations were used. The LDA+U and GGA+U methods require as an input the Coulomb repulsion strength (Hubbard parameter U) and the exchange parameter J which can be related to Slater's integrals [30]. The structure of the VB and CB as well as the bandgap value (E_g) did not change substantially, when calculated using either the LDA+U or GGA+U methods. Thus, significant improvement in the accuracy of the calculated band structure is not expected when employing different DFT methods presently available. The similar conclusion has been done in [31].

The *VB* is composed mainly of 2p states of oxygen with a considerable contribution of 5d states of tungsten in the lower part of the VB starting from the 2.1 eV below the top of the *VB*. The bottom of the *CB* is composed mainly of 5d states of tungsten that form the narrow subband of 0.9 eV width. The subband is separated from the main part of the *CB* by the gap of 0.8 eV. The contribution of electronic states of calcium is negligible in the

Table 1
Atomic positions and lattice parameters in $CaWO_4$.

$CaWO_4$	*Atom*	*x*	*y*	*z*
$a=0.52444$ nm	O	0.1507	0.0086	0.2106
$b=0.52444$ nm	Ca	0	1/4	5/8
$c=1.1381$ nm	W	0	1/4	1/8
$\alpha=90^\circ$, $\beta=90^\circ$, $\gamma=90^\circ$				

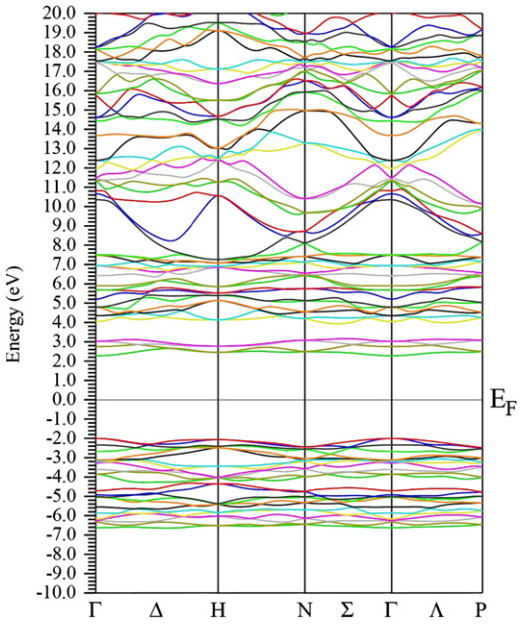

Fig. 1. Band structure of $CaWO_4$.

VB and in the lower part of the *CB*. The considerable contribution of cation 3d states starts at ~3 eV above the bottom of the *CB*.

It is widely known that $CaWO_4$ can be considered as an insulating material or wide-band-gap semiconductor. According to the performed calculation $CaWO_4$ is a direct-gap insulator with the bandgap of 4.1 eV. However the obtained value of the bandgap seems to be underestimated. The band structure problem of a strongly correlated system in DFT associated with LDA and GGA is well-known, they predict band gaps in semiconductors or insulators typically underestimated by 50%. The use of conventional LDA+U or GGA+U methods usually retains the structure of the VB and CB but the bandgap increases. The bandgap is regulated by the selection of the Hubbard parameter U within certain limits (usually 4−7 eV). The first-principles calculation of this parameter is a non-trivial challenge [31]. A possible method to alleviate this problem is to introduce a scissors operator [32]. Assuming that the energy of bandgap must be increased from E_g^{GGA} calculated by the GGA method to $E_g^{GGA}+\Delta$, where Δ is the desirable extension of the bandgap, it is possible to apply this relation in the expression for variational energy. This expression can be solved by the conventional methods. In this work we apply a simpler approach and only shift the DOS calculated by GGA96 at the certain value to obtain the best agreement with experimental data. The necessary experimental data for the comparison with the calculation was obtained measuring the reflectivity of $CaWO_4$.

3.2. Reflectivity of $CaWO_4$

The reflectivity spectra are presented in Fig. 2. It should be noted that the dead surface layer may arise in the oxides that are sensitive to the influence of the environment. In this case the reflectivity from the surface of (*ht*) sample may be distorted as we used the surface of the natural growth. As it was shown, e.g. for the hygroscopic calcium oxide the reflectivity is very sensitive to the quality of the surface of the sample [33]. It was shown that when the surface worsens under the influence of the atmosphere the reflectivity peaks are almost smoothed out. However it is not the case of the calcium tungstate that is chemically resistant and non-hygroscopic compound. The structure of the reflectivity of (*ht*) sample is only slightly less pronounced than that of (*cz*) sample that may be connected to the different quality of the samples itself.

The profiles of the spectra differ substantially—the reflectivity peaks are located at the same energies but the relative intensity of the peaks depend on the sample. As it was shown in [12,13] the anisotropy of the crystal structure of $CaWO_4$ may lead to the essential modification of the reflectivity structure depending on the orientation of the crystallographic axes sample relatively to the electric vector of the incident radiation. The exact orientation of the crystallographic axis of the samples has not been controlled in the present experiment; however, we believe that the difference of the reflectivity structure in the samples under investigation is due to the anisotropy of crystal structure of $CaWO_4$.

Peaks in reflectivity observed below 10 eV were attributed to the transitions from the *VB* formed with 2p O states to the lower part of the *CB* that is formed mainly with 5d *W* states [12,13]. At higher energies (10–15 eV) the contribution from the electronic transitions from the *VB* to the *CB* composed mainly of the calcium states [13] or from the deeper oxygen-related electronic states of the *VB* to the states of the *CB* that are formed with 5d W states [12] is supposed.

It is not the aim of the present work to analyze in details the features of the reflectivity. The obtained reflectivity was used to calculate the permittivity for the further comparison with permittivity obtained from DOS.

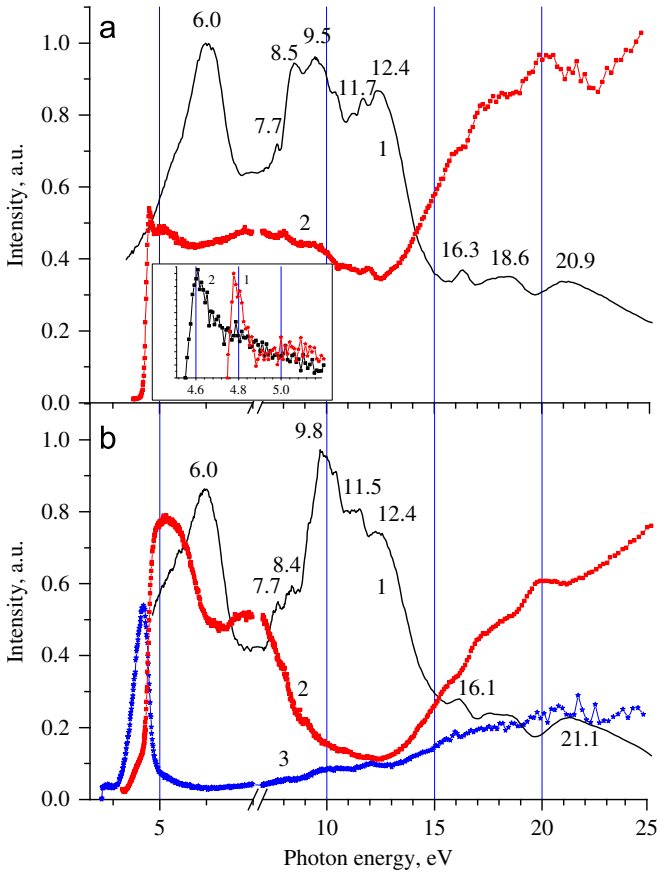

Fig. 2. (a) Reflectivity (1) and luminescence excitation spectra, λ_{em}=440 nm (2) of $CaWO_4$ (*cz*) at T=10 K. In the inset—luminescence excitation spectra in the region of the first sharp peak measured at 10 K (1) and 300 K (2) and (b) Reflectivity (1), and luminescence excitation spectra, λ_{em}=440 nm (2) and λ_{em}=590 nm (3) of $CaWO_4$ (*ht*) at T=10 K. Energy position of the reflectivity peaks is denoted on the plot.

3.3. Calculations of permittivity from DOS experimental reflectivity

The calculations of permittivity were performed using Kramers–Kronig relations. The refractive index of $CaWO_4$ n=1.94 was used as reference parameter in the transparency region. The reflectivity in the region above 25 eV was approximated by $(h\nu)^{-4}$ law. Another parameter for the calculation was the maximum value of the reflection coefficient in the fundamental absorption region R. The measurements of reflectivity performed by us did not allow to obtain information about R from experiment. In order to check the correctness of Kramers–Kronig calculations with given R parameter we used four types of sum rules for partial number of electrons $N(h\nu)$ and zero-frequency dielectric permittivity $\varepsilon(0)$, which are based on $\varepsilon_2(h\nu)$ and energy loss function $\mathrm{Im}(\varepsilon(h\nu)^{-1})$. The calculations of permittivity for the both samples were correct up to the R=30% that was used for the calculations of the optical functions. Generally it is in coincidence with the reflectivity coefficient obtained for $CaWO_4$ in [11] −35%. The "experimental" permittivity calculated in this way was compared with that obtained from the DOS ("theoretical" permittivity).

The theoretical background for calculation of dielectric functions from data of DOS is described in detail in [34,35]. All this formalism has been implemented as a module into the WIEN2k code [25]. The module carries out the Brillouin zone integration and computes the imaginary part of the complex dielectric tensor. The real part of the dielectric tensor is obtained by the Kramers–Kronig relations.

The permittivity curves that were initially obtained from the DOS were significantly shifted to the low-energy region in comparison with that obtained from experimental reflectivity. The discrepancy arises due to underestimation of the bandgap value in the calculated DOS which is a typical problem in case of calculations using full potential LAPW method. In order to get better correspondence between the "theoretical" and "experimental" permittivity curves, the bandgap value was increased: electronic states of the CB were shifted to the higher energies and optical functions were calculated again. The optimal coincidence of the energy position of the first pronounced peak was used as a criterion for the choice of the shift value. Finally the CB shift was 0.8 eV and the bandgap is obtained as 4.9 eV. The real and imaginary parts of dielectric permittivity obtained from Kramers–Kronig analysis of measured reflectivity and those calculated in the framework of density functional formalism are shown in Fig. 3. Since the orientation of the samples was random, for the further analysis we will use "theoretical" permittivity averaged over three directions: $\varepsilon=(\varepsilon_{xx}+\varepsilon_{yy}+\varepsilon_{zz})/3$.

The comparison of "theoretical" and "experimental" permittivity shows that the curves demonstrate a set of common features. First pronounced peak in ε_2 is observed at 6.0 for (*ht*) sample and at 6.1 eV for (*cz*) sample and for the "theoretical" permittivity. In the ε_1 the first peak is observed at 5.62 eV for the "calculated" curve while for the "experimental" curves it was found at 5.77 eV. Therefore the coincidence between the "experimental" and "theoretical" curves is not perfect and the obtained bandgap value should be taken with the certain error 4.9 ± 0.15 eV. The first peak in ε_2 is followed with minimum in the energy region 6.5–8.0 eV with further sharp rise at energies exceeding 8 eV. It is followed by a group of peaks in the region 8.0–10.5 eV and a shoulder at ~11.2 eV with further drop of intensity. The main difference of the structure of ε_2 is observed in the region of the wide non-elementary band in the region 8–10 eV. "Theoretical" ε_2 has two pronounced peaks at 8.8 eV and 9.7 eV, while the "experimental" curves demonstrate only single pronounced peak in this region. For (*cz*) sample the peak is at 8.4 eV followed by the shoulder at 9.3 eV while in (*ht*) sample the peak is at 9.6 eV with the shoulder at lower energies (~8.4 eV). These peaks are the same for both the samples in which relative intensity depends on the orientation of the samples. We suppose that the peaks correspond to the doublet peaking at 8.8 eV and 9.7 eV in the "theoretical" ε_2 that is averaged over three directions. The shift may arise for the following reason. It is known that for any of single-electron approximations including DFT the best result is obtained for DOS located near the top of the VB and the bottom of the CB. However, DFT is not considered accurate enough for calculations which can be used to describe excited states [36]. The peaks observed in the region 8–10 eV correspond to the electronic transitions that involve initial or final electronic states located in the depth of the bands. Therefore the shift between the peaks (0.3–0.4 eV) in "theoretical" and "experimental" ε_2 may be considered as a probe for the joint erroneous shift of the electronic states located in the depth of the VB and CB.

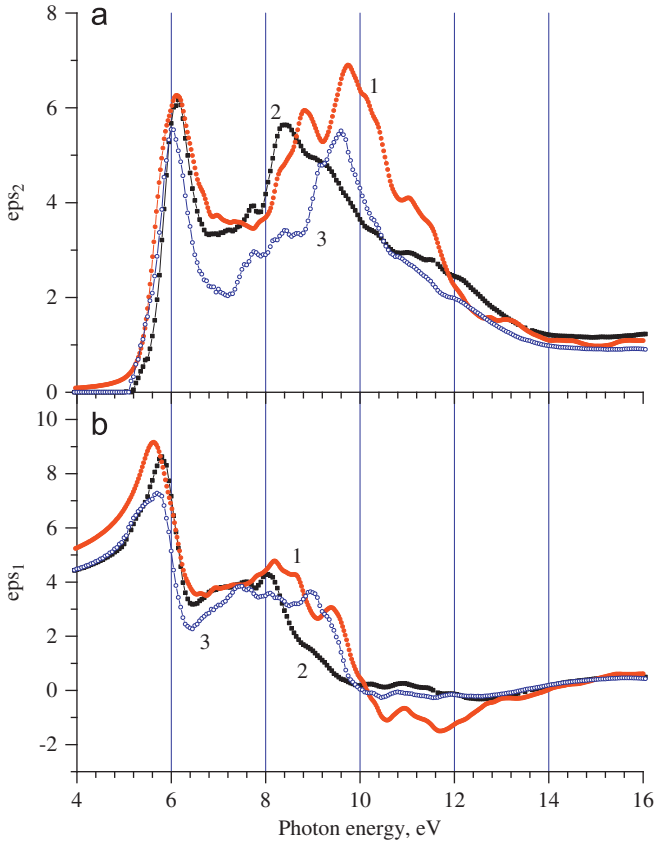

Fig. 3. Real (a) and imaginary (b) parts of permittivity calculated from the DOS (1) and from the experimental reflectivity for (*cz*) (2) and (*ht*) (3) samples.

3.4. The bandgap value of $CaWO_4$.

After the shift of the CB states the bandgap value obtained from the DOS data is $E_g=4.9\pm0.15$ eV. Consistent analysis of experimental data and theoretical calculations implies that the values of basic parameters of $CaWO_4$ like the bandgap value should be in coincidence. Let us analyze the validity of the obtained value from the viewpoint of the results presented in the literature.

Data on the E_g of $CaWO_4$ obtained previously using different experimental and theoretical methods are summarized in Table 2. According to the data presented in the table different experimental and calculation methods allow to get E_g that spread in a wide energy interval 3.9–7.0 eV.

Several theoretical approaches were used for a calculation of the band structure of $CaWO_4$ and its bandgap. The latter varies from 4.09 to 6.5 eV depending on the method applied for the calculations. For theoretical calculations Shao et al. [16] and Itoh [17] used the discrete variational Xα (DV-Xα) method. The Xα method developed by John Slater (1951) usually employed as a standalone exchange functional, without a correlation functional and DV-Xα method is its recent modification. Orhan [15] and Evarestov [18] actually use the same program CRYSTAL98 or CRYSTAL06 respectively. These packages are based on both DFT and Hartree–Fock (HF) theories. Orhan et al. [15] applied the Becke 3-parameter exchange functional and the gradient-corrected correlation functional by Lee, Yang and Parr (B3LYP method). Evarestov et al. [18] used the Becke 3-parameter, Perdew and Wang correlation functional (B3PW method) and the gradient-corrected correlation functional of Perdew, Burke and Ernzerhof (PBE method). Wien code based on the LAPW method was used by Williams [14]. Detailed comparison of different theoretical methods for calculation of strongly correlated electrons requires special consideration and is out of the scope of the present study.

The distinctions in the experimental determination of E_g are connected with experimental methods that were used for this purpose. From the absorption spectra E_g is generally deduced by extrapolation of the absorption edge to zero according to the Wood and Tauc method. For $CaWO_4$ crystals the value of the optical bandgap spreads from 3.9 to 4.94 eV that is obviously depends on the thickness of the sample (see Table 2). The method allows to obtain greater values for the thin films. The values up to 5.27 eV were obtained when the thickness of the samples was reduced to the tens of nanometers (about 100 nm). For the mentioned scale the quantum confinement effects may be expected

Table 2
Bandgap values of $CaWO_4$ obtained using different theoretical and experimental methods.

E_g(eV)	Reference	Remarks
		Data from theoretical calculations
4.09(d)[a]	[14]	DFT, LAPW method
5.27(d)	[15]	HF-DFT, B3LYP method
5.27	[16]	DFT, DV-Xα method
5.97	[17]	DFT, DV-Xα method
6.5(d)	[18]	HF-DFT, B3PW and PBE methods
		Data from absorption
3.87	[4]	Crystal, $d=0.3$ cm
3.94	[43]	Crystalline thin films, $d=1.5$–2.0 mkm
4.6(i)	[42]	Crystal, $d<1$ mm
4.94(d)	[41]	Crystal, $d=10$–30 mkm
5.27	[15,39]	Crystalline thin films, $d=110$ nm
5.4	[40]	Crystalline thin films, $d\sim2$ mkm
		Data on the position of the first reflectivity peak
5.9	[10]	Crystal
6.0	[12]	Crystal
6.0	[44]	Crystal
		Data on the edge of creation of separated e–h pairs
>6.0	[50]	Thermostimulated luminescence excitation
>6.2	[51]	Photoconductivity
6.2–6.5	[9,45,46]	Phosphorescence edge, luminescence excitation
6.8	[47,48]	Thermostimulated luminescence, photostimulated luminescence excitation
7.0	[49]	Thermostimulated luminescence excitation
		Other methods
5.2 ± 0.3	[8]	Two-photon spectroscopy

[a] Type of the bandgap if it was determined—direct (d) ot indirect (i)

that enlarge the bandgap. Even greater value 5.4 eV was obtained for the thicker films in [40] that stand apart from the observed dependence.

The disadvantage of the applied method is that it does not account for the possibility of exciton effects at the edge of the fundamental absorption. Actually in the compounds where excitons are created the E_g exceeds that obtained from the edge of absorption. Some tungstates ($PbWO_4$, $CdWO_4$, $ZnWO_4$) demonstrate typical temperature dependence of the fundamental absorption edge described with empirical Urbach rule that can be considered as a probe for the existence of excitons in tungstates [19,37].

A number of experimental methods that allow to detect the edge of the creation of separated electrons and holes were applied in case of $CaWO_4$. The applied methods that include measurements of photoconductivity, edge of phosphorescence, excitation spectra of thermostimulated and photostimulated luminescence give values of E_g that spread from 6.0 to 7.0 eV. It exceeds the position of the first peak in reflectivity with maximum at 5.9–6.0 eV (see Table 2). Recently it was proved that the peak is of non excitonic origin as it was initially proposed in [9]. The data obtained from the reflectivity indicate that the first peak is due to the band-to-band electronic transitions [13] and the value of the peak maximum gives the upper limit on the E_g. The problem of overestimation of the bandgap value obtained on the basis of experimental data on the edge of separated charge carriers creation in $CaWO_4$ has been the subject of discussion. Current opinion is that the separated charge carriers are created due to the transitions from the 2p O states forming the *VB* to 3d states of Ca that allows spatial separation of electrons and holes [38,45]. Actually the results of the performed calculations indicate that cation states are located in the depth of the *CB* while the bandgap is actually determined by the transitions from the 2p O forming the top of the *VB* to 5d W states that forms the bottom of the *CB*.

The method of two-photon spectroscopy has been also applied for the determination of the bandgap in [8]. The onset of the intrinsic luminescence excitation spectrum has been observed at 2.45 eV under laser excitation with high power density. Implying the two-photon absorption process is responsible for the excitation, the onset of the excitation is obtained by multiplication by factor 2 as 4.9 eV and finally the E_g is estimated by the authors as 5.2 ± 0.3 eV.

In general, the estimation of the bandgap value made on the basis of the present results is in coincidence with the data deduced from the analysis of the absorption of rather thin (several mkm) samples and from the two-photon spectroscopy. The methods that register the effects connected with the creation of separated charge carriers overestimate the bandgap value because separated charge carriers are created when electrons are excited to the higher states of the CB (presumably of calcium origin).

3.5. Luminescence spectra

The luminescence spectra of the investigated samples are presented in Fig. 4. Single luminescence band in the blue spectral region with maximum at 2.83 eV and full width at half maximum (FWHM) 0.79 eV ($T=300$ K) has been observed for $CaWO_4$ (*cz*) sample. The fitting parameters of luminescence spectra with Gauss curves are presented in Table 3. The peak slightly shifts to the low-energy region and becomes narrower with cooling of the crystal from 300 K down to 10 K. No luminescence signal was detected under excitation below the fundamental absorption region (4.5 eV) at $T=10$ K. Two luminescence bands were found in the $CaWO_4$ (*ht*) sample. The band in the blue spectral region is similar to that observed for (*cz*) sample while the second one is a luminescence band in the green spectral region with maximum at 2.23 eV and FWHM 0.61 eV ($T=10$ K). The band is excited separately in the region below the fundamental absorption edge. When excitation energy exceeds the fundamental absorption edge the high-energy band also contributes into the overall spectrum.

The observed luminescence bands are well known and described e.g. in [3–8,11]. The "blue" band represents the intrinsic emission of $CaWO_4$ and is usually attributed to radiative transitions within the WO_4^{2-} complex with possible creation of the self-trapped excitons [4,11,14]. The "green" band is due to the radiative relaxation on the structural defects of $CaWO_4$, usually the emission center is attributed to the extrinsic oxyanion groups with oxygen vacancy —WO_3 complexes [5,52].

From the luminescence data follows that the quality of (*cz*) sample is better than that of (*ht*) sample that contains defects of crystal structure responsible for the "green" emission band. Therefore below we will analyze the processes of the energy transfer to the emission centers for the $CaWO_4$ crystals with considerably different quality. It results in the considerable competition with defect-related radiative (and possible non-radiative) relaxation channel in (*ht*) sample whereas in (*cz*) sample the competition is considered as negligible.

3.6. Luminescence excitation spectra of $CaWO_4$

The luminescence excitation spectra measured in the fundamental absorption region provide information about the efficiency of the energy transfer to the emission centers. The excitation spectra of intrinsic and defect-related luminescence measured at $T=10$ K in (*ht*) sample are presented in Fig. 2(b). Different character of the energy transfer to the emission centers related to self-trapped

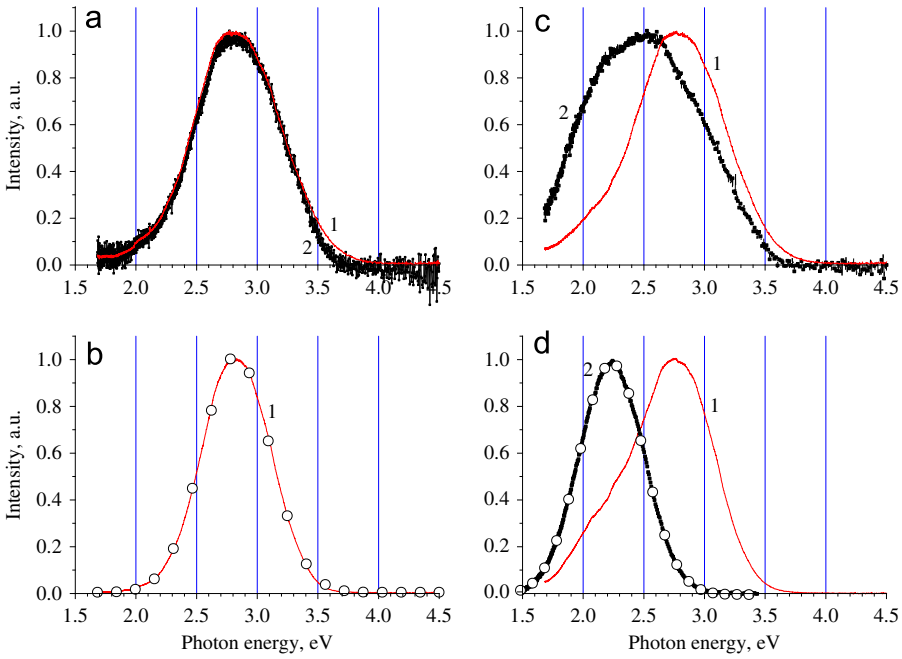

Fig. 4. Luminescence of $CaWO_4$ (*cz*) sample at $T=300$ K (plot *a*) and $T=10$ K (plot *b*) and $CaWO_4$ (*ht*) sample at $T=300$ K (plot *c*) and $T=10$ K (plot *d*). Excitation energy was 11.0 eV for the curves denoted as (1) and 4.5 eV for the curves denoted as (2). The fitting with a single Gauss curves is presented at plots (b) and (d) for the both observed emission bands (hollow dots).

Table 3
Parameters of luminescence spectra fitting with Gauss curves for $CaWO_4$ (*cz*) and (*ht*) samples. $E_{1,2}$ is the position of the band's maxima, $FWHM_{1,2}$—its full width on the half maximum. In brackets the weight of the defect-related emission band relatively to the intrinsic band is presented.

	E_1,eV	$FWHM_1$,eV	E_2,eV	$FWHM_2$,eV
(cz)sample				
$E_{ex}=4.5$ eV, $T=300$ K	2.83	0.79	No emission	
$E_{ex}=11.0$ eV, $T=300$ K	2.83	0.79	No emission	
$E_{ex}=4.5$ eV, $T=10$ K	No emission		No emission	
$E_{ex}=11.0$ eV, $T=10$ K	2.82	0.75	No emission	
(ht)sample				
$E_{ex}=4.5$ eV, $T=300$ K	2.78	0.81	2.17(90%)	0.66
$E_{ex}=11.0$ eV, $T=300$ K	2.81	0.79	2.13(9%)	0.66
$E_{ex}=4.5$ eV, $T=10$ K	No emission		2.23	0.61
$E_{ex}=11.0$ eV, $T=10$ K	2.8	0.75	2.23(32%)	0.61

excitons and to the defects of the crystal structure determines the behavior of the spectra [48]. The first peak in the excitation spectrum of intrinsic luminescence is observed at 5.2 eV that corresponds to interband electron transitions according to the present estimation of E_g. The peak is followed by the second peak at 6.9 eV with the further gradual decrease of the intensity up to the energies corresponding to the edge of the photon multiplication process (~13 eV). The behavior is typical for the exciton mechanism of the energy transfer to the emission centers, i.e. the center captures charge carriers that were already bound into exciton. The pronounced decrease of the intensity up to the energies of photon multiplication testifies to the presence of the strong competitive relaxation center, such as extrinsic luminescence center.

For the extrinsic luminescence the behavior of excitation spectrum considerably differs. The pronounced peak at 4.6 eV corresponds to the region behind the fundamental absorption edge and is attributed to the direct excitation of the defect states located in the forbidden band of $CaWO_4$. In the region of the fundamental absorption the intensity of excitation gradually increases starting from the ~7 eV that correspond to the edge of the separated e–h pairs creation (see Table 2). Such behavior characterizes the recombination type of energy transfer to the luminescence centers, i.e. the charge carriers are sequentially captured on the emission center.

The structure with the double peak in the low energy region of the excitation spectrum of intrinsic emission is commonly observed in $CaWO_4$. It has been demonstrated in several papers for the powders and crystals of $CaWO_4$ [9,44–47]. However it was also shown that the spectrum profile may vary that is depend on the treatment conditions of the samples [56].

The excitation spectrum of intrinsic luminescence in (*cz*) sample is presented in Fig. 2(a) and it is considerably differs from that of (*ht*) sample.

The sharp and narrow peak is observed at 4.77 eV. Apparently it is located below the bandgap and might be the manifestation of the excitons creation in $CaWO_4$. The observation of the creation of excitons in tungstates with a scheelite crystal structure is a non-trivial problem. Initially the first peak in the reflectivity at 6.0 eV was attributed to the manifestation of the excitons in $CaWO_4$ [9]. However, later it was shown that the peak is due to the band-to-band transitions [13]. The peak is also reproduced in the optical function calculated from DOS (Fig. 3) that should not happen if it is of excitonic origin since the calculations do not account for the excitonic effects. The absence of the excitonic peak in reflectivity have been also demonstrated for the other crystals with scheelite structure—$SrWO_4$ and $BaWO_4$ [44,53]. Only in the $PbWO_4$ the exciton is clearly observed in the reflectivity in the region of fundamental absorption edge. However its origin is connected with the participation of cation electronic states in the formation of the top of the valence band and the bottom of the conduction band [44,54] that is not the case in other tungstates with scheelite crystal structure. Therefore the low oscillator strength has been proposed as the explanation of the absence of the excitons in $CaWO_4$ in [13]. It is rather unusual taking into account that $CaWO_4$ is the compound with the direct gap. The reason of the very low oscillator strength for the excitonic transition in scheelites is not clear.

The existence of the excitons in tungstates may be also deduced from the luminescence excitation spectra. In (*cz*) sample we have observed the sharp feature with maximum at the 4.77 eV. The feature is not artificial since it was already observed in [56] for some samples of $CaWO_4$ obtained after certain treatment. The temperature dependence of this peak has not been investigated. We have measured the excitation spectra for (*cz*) sample at 10 K and also at 300 K (see the inset in Fig. 2). As it follows from the figure the peak as well as the low energy edge is shifted to the low energy region with the increase of the temperature that is due to the shift of the Urbach tail of the fundamental absorption region. The peak is very narrow, however its profile becomes broader with the temperature increase -0.07 eV at $T=10$ K and 0.1 eV at $T=300$ K. Very similar manifestation of the excitons in the excitation spectra has been found in another complex oxide—LUAP:Ce [55]. In this compound the existence of the excitons can be deduced directly from data on the reflectivity. The width of the corresponding excitonic peak observed in the luminescence excitation spectra is about 0.08 eV. Hence we can expect the similar manifestation of excitons in other complex oxides. The discussion presented above allows to suppose that this peak represents the manifestation of excitons in $CaWO_4$. However additional dedicated study is required to clarify the question of the excitons creation in the scheelites.

The sharp peak at 4.77 eV is absent in (*ht*) sample probably because of the presence of local defect related states in the vicinity of the *CB* and *VB* edges. These states are responsible for the peak at 4.6 eV and may prevent the creation of the exciton in (*ht*) sample.

Different behavior of the excitation spectra of (*ht*) and (*cz*) samples may be connected with the distortions of the band structure in (*ht*) sample that is perturbed due to the lower quality of the crystal. The possible influence on the band structure of the different defects connected with oxygen (vacancies, interstitial oxygen) has been considered in the [16,57] for $CaWO_4$ and also for the $CaMoO_4$ that commonly demonstrate similar optical properties. As it follows from the results of the calculations the main changes in DOS occurs in the region of the vicinity of the bandgap where additional peaks arise while the regular structure changes very slightly. The possible perturbation of the band structure in the (*ht*) sample may be deduced from the reflectivity spectra. However, it was not observed in the region of the first reflectivity peak where the most considerable changes are expected since the main modification of DOS occurs in the region of fundamental absorption edge. In the fundamental absorption region the position of the reflectivity peaks for the (*ht*) sample is generally the same as for the more perfect (*cz*) sample. The relative intensity of the peaks differs in these samples due to the different orientation as discussed above. Therefore the perturbations of DOS are not so considerable to be observed in the reflectivity. The excitation spectra may be more sensitive to the perturbations of the band structure. Actually the additional structure in DOS that arises in the vicinity of the bandgap may be manifested as the peak in the excitation spectrum of the "green" emission band that is observed below the fundamental absorption edge.

The perturbation of the band structure in the fundamental absorption edge is not so much considerable to be the reason of the substantial difference between the excitation spectra of the intrinsic emission in (*ht*) and (*cz*). To our opinion the different quality of the samples yields in the modification of the relaxation processes and energy transfer to the emission centers. The decrease of intensity in the excitation of (*cz*) sample in the region 6–12 eV is much less pronounced in comparison to that in (*ht*) sample. In (*ht*) sample energy transfer to intrinsic emission center is accompanied by the competition with the energy transfer to the defect emission center. With the increase of excitation energy the energy transfer becomes more efficient to the defect-related center and hence it becomes less efficient to the intrinsic emission center. As in (*cz*) sample the competition with the defect related emission center is absent the decrease in the excitation spectrum is not considerable.

The origin of the features observed in the excitation spectra may be analyzed using the data of the DOS calculations as it was shown in [23] for the case of $ZnMoO_4$. In the next part we are going to analyze the possible correlations in DOS and excitation spectra.

3.7. Correlations between DOS and luminescence excitation spectra

For the further analysis of intrinsic luminescence excitation spectra we will exclude the possible modification of the excitation spectra with energy losses on the reflectivity. The energy losses are proportional to the value of reflectivity at given energy because the part of excitation photons are reflected from the crystal and does not participate in the process of luminescence. Therefore the behavior of reflectivity may result in modulation of the excitation spectra. It is especially important for the anisotropic crystals where the anisotropy of the crystal structure influence on the reflectivity spectra profile. It may introduce additional distortions into the profile of the excitation spectra of the studied samples of $CaWO_4$ since the orientation of the samples was different. The possible distortions that arise due to this factor are accounted, when we corrected the excitation spectra on the factor of the energy losses on the reflectivity. Hence the performed correction also excludes the possible distortion of the excitation spectra connected with the anisotropy of the crystal structure that is manifested in the reflectivity.

In Fig. 5 we present the excitation spectra corrected for the reflectivity with the absolute values that were used previously for the calculations of permittivity. When the correction on reflectivity losses is done some features in excitation spectra are smoothed

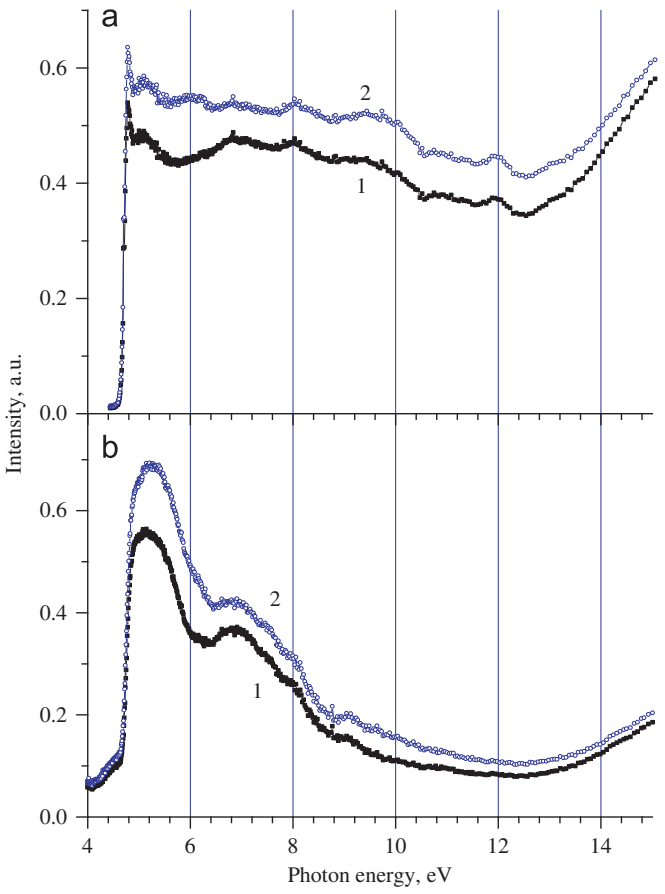

Fig. 5. Luminescence excitation spectra of $CaWO_4$, (*cz*) sample (a) and (*ht*) sample (b) without correction on reflectivity (1) and corrected on reflectivity (2).

out, e.g. the minimum at 5.8 eV in (*cz*) sample. In the excitation spectra of (*ht*) the observed first minimum at 6.25 is much more pronounced then that in (*cz*) sample. It was not smoothed out when the correction on the reflectivity losses is performed. As a result two obvious large bands at 5.2 eV (band A) and 6.8 eV (band B) and a hump at 9.2 eV (band C) are observed for (*ht*) sample.

The structure with the two distinctive peaks in the low-energy region is commonly observed in the excitation spectra of tungstates and also of molybdates that demonstrate very similar luminescence properties. Beside $CaWO_4$ similar dependence of the excitation spectra have been observed for $SrWO_4$ [53], Li_2WO_4 [38], $CaMoO_4$ [58] and $ZnMoO_4$ [23]. In the latter case the structure in the excitation spectra has been analyzed using the data of the calculated DOS. It was assumed that the relation between the excitation spectra and the DOS of a crystal is a non-trivial problem that requires careful analysis. Not only the band structure itself, but also the processes of excitation energy transfer to the emission centers should be taken into account. Using calculated partial absorption spectra it was demonstrated that the observed doublet in excitation spectra is due to electronic transitions from the top of the *VB* to the lower part of the *CB* formed mainly with d states of Mo. The latter is divided into two subbands that is due to E–T splitting of Mo 4d states in tetrahedral crystal field [23]. As far as the similar splitting may be expected for the set of crystals with tetrahedral oxyanion WO_4 (or MoO_4) the doublet observed in their excitation spectra may be also connected with the features of *CB* structure.

In Fig. 6 the excitation spectra of intrinsic emission are combined together with the partial DOS of $CaWO_4$. The E_g of the calculated DOS was shifted on 0.8 eV in order to get the agreement between the energy position of the first peak in permittivity spectra obtained from DOS and from experimental reflectivity as it was described in 3.2. Only main *p*-like states for oxygen and *d*-like states for calcium and tungsten are presented in Fig. 6. The VB of $CaWO_4$ mostly consists from O 2p states. The CB (right side in Fig. 6) is divided into two parts. The lower part of *CB* (from 4 to 8 eV) is mainly composed of W 5d states and the upper CB (8–10 eV) involves contribution mainly from Ca 3d states. The comparison helps us to identify and explain the nature of excitation bands and to verify whether the bandgap of $CaWO_4$ was determined correctly.

The correlation between the CB DOS and excitation spectrum is clearly observed for (*ht*) sample (Fig. 6, curve 2a). The low-energy peaks are due to the transitions within WO_4 complex because the electronic states of oxygen and tungsten form the top of the *VB* and bottom of the CB. The WO_4^{2-} groups can absorb excitation energy through $O^{2-} \rightarrow W^{5+}$ host charge transfer transition. The band A is associated with transitions from 2p-like states of O to *W* 5d states that form the lower subband of the *CB*. The band B is a hybrid band and it is composed from [O→W] charge transfer transitions and the high-energy part probably also from transitions to calcium states. The band C is also related to the host absorption, probably to the transitions which involves mostly the transitions between 2p-like states of O and 3d-like states of Ca or O^2–Ca^{2+} charge transfer transition.

The assumption on the nature of the band C is further confirmed by calculation of the position of the band C that can be also performed with the help of an empirical formula given by Jorgensen [59]:

$$E_{CT} = [(X) - (M)] \times 30{,}000\,\mathrm{cm}^{-1}$$

Here E_{CT} gives the position of the host charge transfer (HCT) band in cm^{-1}, (X) is the optical electronegativity of the anion, and (M) is the same for the central metal ion. Using Pauling scale for electronegativity [60], namely (O)=3.44 and (Ca)=1.00, the HCT of Ca–O, can be estimated near the 73,000 cm^{-1}, or around 9.05 eV. The obtained value is close to the position of the band C—9.2 eV.

Electronic transitions from the VB to the states of tungsten and calcium completely explain the nature of all three bands in excitation spectra of (*ht*) sample. The possible error of the energy position of the DOS located in the depth of the bands was deduced in the part 3.3. However the possible shift of the electronic states on 0.3–0.4 eV does not lead to a considerable mismatch of the broad bands in excitation spectra and the CB DOS.

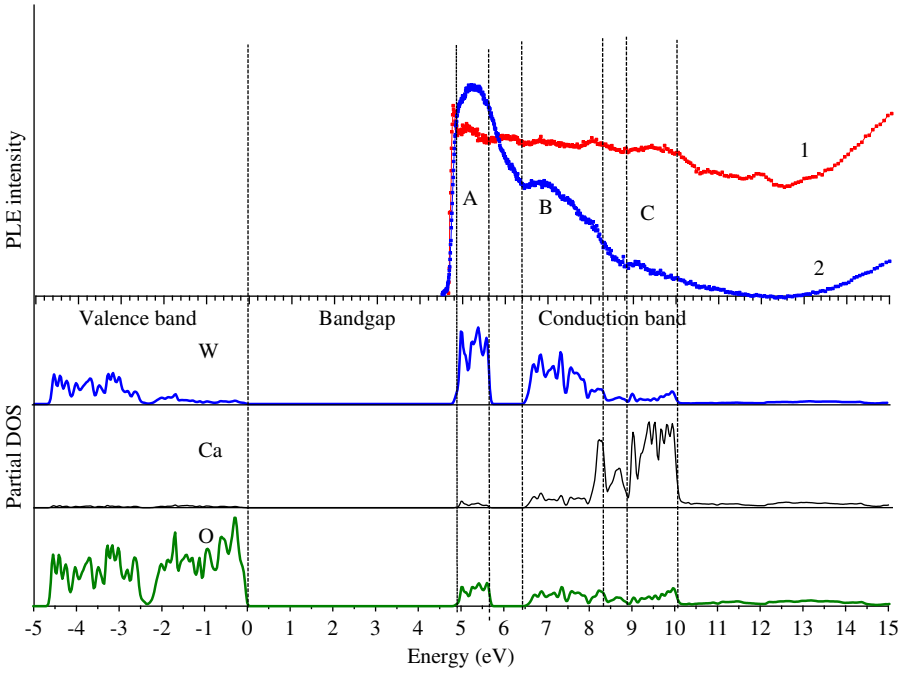

Fig. 6. Luminescence excitation spectra (λ_{em}=440 nm, T=10 K), corrected on reflectivity for the (*cz*) sample (1) and (*ht*) sample (2). The partial density of states of *W*, Ca and O are presented below.

If the observed correlation between the DOS of the *CB* and excitation spectra is not accidental it should mean that the radiative relaxation on intrinsic emission center is mostly probable for excitations with initial states located near the top of the *VB*. Electronic transitions with the initial states located in the deep of the *VB* have less probability to be captured by the intrinsic emission center, otherwise all three band should be smoothed out or shifted to the high-energy region. It leads to the conclusion that the high-energy holes are intercepted by other (radiative and non-radiative) channels during thermalization and this process is more probable for high-energy holes then for high-energy electrons. The competitive defect-related radiative relaxation channel really exists in (*ht*) sample.

We also tried to find correlations between the excitation spectra and the states of the *VB*. No obvious correlation between the excitation spectra and the states of the *VB* was found. The *VB* consist of two subbands with a distinct minimum between them at -2.35 eV. The first excitation peak for (*ht*) sample is considerably narrower then the width of the upper subband of the *VB*. It indicates on the minor role of the transitions from the depth of the *VB* to the lower states the *CB* in the energy transfer to intrinsic emission centers.

The correlation between the DOS and the excitation spectrum of intrinsic luminescence in (*cz*) sample was not observed. Actually the intensity in the excitation spectrum fluctuates around the constant level from the start of the interband transitions up to the 10 eV and all the features are smoothed out. We suppose that the absence of the correlation between DOS and features in excitation spectrum of (*cz*) sample is due to the high probability of radiative relaxation for electrons not only from the very top of the valence band but also from the deeper states of the *VB* and from the top of the *VB* to 3p Ca states. It is determined by the better quality of the sample that results in the minor role of the competitive defect-related relaxation channels.

4. Conclusions

The calculations of the band structure of $CaWO_4$ were performed in the framework of DFT using the full potential LAPW method. The position of the CB DOS was corrected using experimental data on reflectivity. The bandgap E_g of $CaWO_4$ was determined as 4.9 ± 0.15 eV. The correlation between the CB DOS and the excitation spectrum of intrinsic luminescence is clearly observed for the sample of $CaWO_4$ with a considerable concentration of the crystal structure defects that give rise to the extrinsic emission band. The existence of the competitive to intrinsic relaxation channel that intercepts predominantly the high energy holes is responsible for the observed correlation. For the high-quality sample of $CaWO_4$ the correlation between the DOS and the excitation spectrum is absent due to the high probability of radiative relaxation for charge carriers from the deep of the *VB* and *CB* determined by the minor role of the competitive defect-related channels.

Acknowledgments

Financial support of grants of the Federal Agency of Science and Innovations no. 02.740.11.0546, BMBF Project RUS 10/037 and RFBR 11-02-01506-a is gratefully acknowledged. We are grateful to Prof. G. Zimmerer for providing the opportunity to perform measurements at the SUPERLUMI station and to Dr. G. Stryganyuk and Dr. A. Kotlov for their assistance during the measurements. We are also grateful to Dr. L. Iskhakova for providing the X-ray phase analysis data and to Prof Yu. Zorenko and Dr. L. Potkin for providing us with the samples of $CaWO_4$.

References

[1] Yu.G. Zdesenko, F.T. Avignone III, V.B. Brudanin, F.A. Danevich, V.V. Kobychev, B.N. Kropivyansky, S.S. Nagorny, V.I. Tretyak, Ts. Vylov, Astroparticle Phys. 23 (2005) 249–263.
[2] V.B. Mikhailik, H. Kraus, S. Henry, A.J.B. Tolhurst, Phys. Rev. B 75 (2007) 184308.
[3] H.F. Hameka, C.C. Vlam, Physica, 1953 943-949.
[4] M.J. Treadway, R.C. Powell, J. Chem. Phys. 61 (1974) 4003–4011.
[5] R. Grasser, A. Scharmann, J. Lumin. 12/1 (3) (1976) 473–478.
[6] G. Blasse, B.C. Grabmaier, Lumin. Mater., Springer-Verlag, Berlin/Heidelberg/New York, 1994.
[7] M. Pashkovskii, L. Limarenko, A. Nosenko, Influence of the structural defects on physical properties of the tungstates, Vysshaya shkola, 1978. (in Russian).
[8] V.B. Mikhailik, H. Kraus, D. Wahl, M. Itoh, M. Koike, I.K. Bailiff, Phys. Rev. B 69 (2004) 205110.
[9] A.M. Gurvich, E.R. Ilmas, T.I. Savikhina, M.I. Tombak, Zhurnal Prikladnoi Spectroscopii 14 (1971) 1027–1031, in Russian.
[10] R. Grasser, E. Pitt, A. Scharmann, G. Zimmerer, Phys. Status Solidi (b) 69 (1975) 359–368.
[11] E.G. Reut, AN Izvestiya, SSSR, Seriya Fizicheskaya 49 (1985) 2032–2038, in Russian.
[12] I.A. Kamenskikh, V.N. Kolobanov, V.V. Mikhailin, I.N. Shpinkov, D.A. Spassky, G. Zimmerer, L.I. Potkin, B.I. Zadneprovsky, Nucl. Instrum. Methods A 470 (1–2) (2001) 270–273.
[13] M. Fujita, M. Itoh, S. Takagi, T. Shimizu, N. Fujita, Phys. Status Solidi (b) 243 (2006) 1898–1907.
[14] Y. Zhang, N.A.W. Holzwarth, R.T. Williams, Phys. Rev. B 57 (1998) 12738–12750.
[15] E. Orhan, M. Anicete-Santos, M.A.M.A Maurera, F.M. Pontes, A.G. Souza, J. Andres, A. Beltran, J.A. Varela, P.S Pizani, C.A. Taft, E. Longo, J. Solid State Chem. 178 (2005) 1284–1291.
[16] Z. Shao, Q. Zhang, T. Liu, J. Chen, Phys. Status Solidi (a) 204 (9) (2007) 3159–3164.
[17] M. Itoh, N Fujita, Y Inabe, J. Phys. Soc. Jpn. 75 (2006) 084705.
[18] R.A. Evarestov, A. Kalinko, A. Kuzmin, M. Losev, J. Purans, Integrated Ferroelectrics 108 (2009) 1–10.
[19] V. Nagirnyi, M. Kirm, A. Kotlov, A. Lushchik, L.J. onsson, J. Lumin. 102–103 (2003) 597–603.
[20] Y. Abraham, N.A.W. Holzwarth, R.T. Williams, Phys. Rev. B 62 (2000) 1733–1741.
[21] Y. Zhang, N.A.W. Holzwarth, R.T. Williams, M. Nikl in: R.T. Williams, W.M. Yen (Eds.), Excitonic Processes in Condensed Matter, PV 98-25, The electrochemical Society Proceedings Series, Pennington, NJ, 1998, pp. 420–425.
[22] N.A.W. Holzwarth, Y. Zhang, R. Williams, in: Proceedings of the International Workshop on Tungstate Crystals, Roma, October 12–14, 1998, pp.101–114.
[23] D.A. Spassky, A.N. Vasil'ev, I.A. Kamenskikh, V.V. Mikhailin, A.E. Savon, Yu.A. Hizhnyi, S.G. Nedilko, P.A. Lykov, J. Phys.: Condens. Matter 23 (2011) 365501.
[24] G. Zimmerer, Rad. Meas. 42 (2007) 859–864.
[25] P. Blaha, K. Schwarz, G.K.H. Madsen, D. Kvasnicka, J. Luitz, in: K. Schwarz (Ed.), WIEN2k, An Augmented Plane Wave+Local Orbitals Program for Calculating Crystal Properties, User's Guide, Vienna University of Technology, 2001.
[26] J.P. Perdew, K. Burke, M. Ernzerhof, Phys. Rev. Lett. 77 (1996) 3865.
[27] V.D. Zhuravlev, M.Y. Khodos, Y.A. Velikodnyi, Russ. J. Inorg. Chem. 37 (1992) 264–266.
[28] A.G. Petukhov, I.I. Mazin, L. Chioncel, A.I Liechtenstein, Phys. Rev. B 67 (2003) 153106.
[29] F. Tran, P. Blaha, K. Schwarz, P. Novák, Phys. Rev. B 74 (2006) 155108.
[30] I.V. Solovyev, P.H. Dederichs, V.I. Anisimov, Phys. Rev. B 50 (1994) 16861.
[31] J. Hölsä, T. Laamanen, M. Lastusaari, M. Malkamäki, P. Novák, J. Lumin. 129 (2009) 1606–1609.
[32] Z.H. Levine, D.C. Allan, Phys. Rev. Lett. 63 (1989) 1719.
[33] C Lushchik, E Feldbach, A Frorip, M Kirm, A Lushchik, A Maaroos, I Martinson, J. Phys.: Condens. Matter 6 (1994) 11177.
[34] R. Abt, C. Ambrosch-Draxl, P. Knoll, Physica B 194-196 (1994) 1451–1452.
[35] C. Ambrosch-Draxl, J. Sofo, Comput. Phys. Commun. 175 (2006) 1.
[36] T. Ziegler, Chem. Rev. 91 (1991) 651–667.
[37] M. Itoh, H. Yokota, M. Horimoto, M. Fujita, Y. Usuki, Phys. Status Solidi (b) 231 (2002) 595–600.
[38] V. Nagirnyi, P. Dorenbos, E. Feldbach, L. Jönsson, M. Kerikmäe, M. Kirm, E. van der Kolk, A. Kotlov, H. Kraus, A. Lushchik, V. Mikhailik, R. Sarakvasha, A. Watterich, in: Proceedings of the 8th International Conference on Inorganic Scintillators and Their Use in Scientific and Industrial Applications, September 19–23, 2005, Alushta, Ukraine, p. 36–40.
[39] M.A.M.A. Maurera, A.G. Souza, L.E.B. Soledade, F.M. Pontes, E. Longo, E.R. Leite, J.A. Varela, Mater. Lett. 58 (2004) 727–732.
[40] N. Saito, A. Kudo, T. Sakata, Bull. Chem. Soc. Jpn. 69 (1996) 1241–1245.
[41] R. Lacomba-Perales, J. Ruiz-Fuertes, D. Errandonea, D. Martinez-Garcia, A. Segura, EPL 83 (2008) 37002.

[42] S.K. Arora, B. Chudasama, Cryst. Res. Technol. 41 (2006) 1089.
[43] Z. Lou, M. Cocivera, Mater. Res. Bull. 37 (2002) 1573–1582.
[44] V.N. Kolobanov, I.A. Kamenskikh, V.V. Mikhailin, I.N. Shpinkov, D.A. Spassky, B.I. Zadneprovsky, L.I. Potkin, G. Zimmerer, Nucl. Instrum. Methods A 486 (2002) 496–503.
[45] A.M. Gurvich, B.N. Meleshkin, V.V. Mikhailin, A.G. Hundzhua, Zhurnal Prikladnoi Spectroscopii 20 (1974) 645–648, in Russian.
[46] A.M. Gurvich, V.B. Gutan, B.N. Meleshkin, V.V. Mihailin, A.A. Mikhalev, M.I. Tombak, J. Lumin. 15 (1977) 187–199.
[47] V. Nagirnyi, E. Feldbach, L. Jonsson, M. Kirm, A. Kotlov, A. Lushchik, L.L. Nagornaya, V.D. Ryzhikov, G. Svensson, I.A. Tupitsina, M. Asberg-Dahlborg, in: Proceedings of International Workshop on Tungstate Crystals, Roma, October 12–14, 1998, pp.155–159.
[48] V. Nagirnyi, E. Feldbach, L. Jonsson, M. Kirm, A. Lushchik, Ch. Lushchik, L.L. Nagornaya, V.D. Ryzhikov, F. Savikhin, G. Svensson, I.A. Tupitsina, Radiat. Meas. 29 (1998) 247–250.
[49] V. Murk, M. Nikl, E. Mihokova, K. Nitsch, J. Phys. Condens. Matter 9 (1997) 249–256.
[50] V. Murk, B. Namozov, N. Yaroshevich, Radiat. Meas. 24 (1995) 371–374.
[51] W. Huber, E. Pitt, A. Scharmann, Zeitschrift für Naturforschung A 27 (1972) 1377.
[52] R. Grasser, W. Pompe, A. Scharmann, J. Lumin. 40&41 (1988) 343–344.
[53] S.N. Ivanov, I.V. Kitaeva, V.N. Kolobanov, V.V. Mikhailin, D.A. Spassky, L.I. Ivleva, I.S. Voronina, B.I. Zadneprovski, Izvestia VUZOV. Fizika 49 (2006) 44–48.
[54] M. Itoh, M. Fujita, Phys. Rev. B 62 (2000) 12825–12830.
[55] V. Kolobanov, V. Mikhailin, N. Petrovnin, D. Spassky, Yu. Zorenko, Phys. Status Solidi (b) 243 (2006) R60–R62.
[56] V. Yakovyna, Ya. Zhydachevskii, V.B. Mikhailik, I. Solskii, D. Sugak, M. Vakiv, Opt. Mater. 30 (2008) 1630–1634.
[57] Y.B. Abraham, N.A.W. Holzwarth, R.T. Williams, G.E. Matthews, A.R. Tackett, Phys. Rev. B 64 (2001) 245109.
[58] V.B. Mikhailik, H. Kraus, D. Wahl, M.S. Mykhaylyk, Phys. Status Solidi (b) 242 (2005) R17–R19.
[59] C.K. Jorgensen, Prog. Inorg. Chem. 12 (1970) 101–158.
[60] L. Pauling, Nature of the Chemical Bond, third ed., Cornell University Press, NY, 1960.